FIRST PRINCIPLE FLUID MODELLING OF NEOCLASSICAL TEARING MODES AND OF THEIR CONTROL

P. Maget[1], O. Février[1], X. Garbet[1], G. Giruzzi[1], H. Lütjens[2], J-F Luciani[2], P. Beyer[3], J. Decker[4], O. Sauter[4], E. Lazzaro[5], S. Nowak[5], M. Reich[6], the ASDEX Upgrade team and the EUROfusion MST1 Team*

[1] CEA, IRFM, F-13108 Saint Paul-lez-Durance, France. [2] Centre de Physique Théorique, Ecole Polytechnique, CNRS, 91128 Palaiseau, France. [3] Aix-Marseille Université, CNRS, PIIM UMR 7345, 13397 Marseille Cedex 20, France. [4] Swiss Plasma Center, Ecole Polytechnique Fédérale de Lausanne (EPFL), Centre de Recherches en Physique des Plasmas, Station 13, CH-1015 Lausanne,Switzerland. [5] Istituto di Fisica del Plasma P.Caldirola, CNR, Milano, Italy. [6] Max Planck Institut für Plasmaphysik, Boltzmannstraβe 2, D-85748 Garching, Germany.

*See appendix of H. Meyer et.al. (OV/P-12) Proc. 26th IAEA Fusion Energy Conf. 2016, Kyoto, Japan

Summary

- A self-consistent fluid drift-neoclassical model has been implemented in the XTOR-2F full MHD code [1,2]
  - Recovers standard neoclassical theory at equilibrium
  - Evidence of island filamentation at low dissipation
  - Bootstrap contribution mitigated by ExB flow
- Island control by ECCD is modelled [5,6]
  - Stabilization efficiency vs source width & misalignment
  - Flip instability and RF-driven island (if 3D source & no rotation)
  - Control strategies mitigating misalignment & broad source

Drift-neoclassical model and insights on NTM drive

Nonlinear MHD code XTOR-2F [1] : drift fluid 3D full MHD in a torus.
Neoclassical model [2] : ion flow and bootstrap arise from friction forces

$$\rho\left(\partial_t + \mathbf{V}\cdot\nabla\right)\mathbf{V} = -\rho\mathbf{V}_i^*\cdot\nabla\mathbf{V}_\perp + \mathbf{J}\times\mathbf{B} - \nabla p - \nabla\cdot\Pi_\parallel + \nabla\cdot\nu\nabla\mathbf{V}_i$$

$$\mathbf{E} + \mathbf{V}\times\mathbf{B} = \eta\left[\mathbf{J} - \mathbf{J_{bs}} - \mathbf{J_{CD}}\right] - d_i\frac{\nabla_\parallel p_e}{\rho}$$

$$J_{bs} = \frac{\eta - \eta_{SP}}{\eta}\left[J_\parallel + \frac{d_i}{\rho}\frac{3/2\pi_{\parallel e}}{(\eta-\eta_{SP})}\nabla\cdot\mathbf{b} - \alpha_e\frac{d_i}{\eta-\eta_{SP}}\sum_s \Lambda_{12}^{es}\frac{u_{2\parallel,s}}{B}\right] \quad \text{: bootstrap current}$$

$$\Pi_\parallel = \frac{3}{2}\pi_\parallel\left[\mathbf{bb} - \frac{1}{3}\mathbf{I}\right] \quad \text{: stress tensor in CGL form}$$

$$\frac{3}{2}\pi_{\parallel,s} = -\rho\alpha_s\mu_s C\left\{\left[\mathbf{V}_s + k_s\left(\mathbf{V}_{Ts}^* + \frac{u_{\parallel 2,s}}{B^2}\mathbf{B}\right)\right]\cdot\nabla\ln B + \frac{\mathbf{b}}{B}\cdot\left[\nabla\times(\mathbf{V}_s\times\mathbf{B}) + k_s\nabla\times(\mathbf{V}_{Ts}^*\times\mathbf{B})\right] - k_s\mathbf{V}_{Ts}^*\cdot\nabla\ln p_s\right\} \quad \text{: pressure anisotropy } (p_{//}-p_\perp)$$

Main properties

- Equilibrium flux averaged bootstrap current consistent with neoclassical theory [3]
- Agrees with analytical estimates [4]; contribution from parallel heat flows [fig.1]
- Non linear saturation is bursty at low dissipation (χ, ν) [fig.2]
- Island shape : droplet like due to drift physics [fig.3]

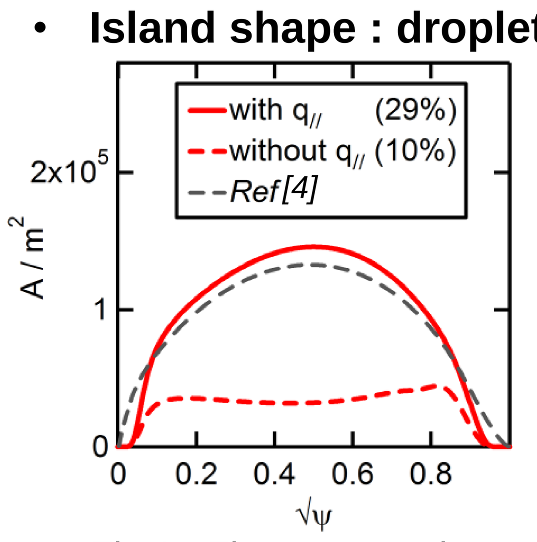

Fig.1 : Flux averaged bootstrap current

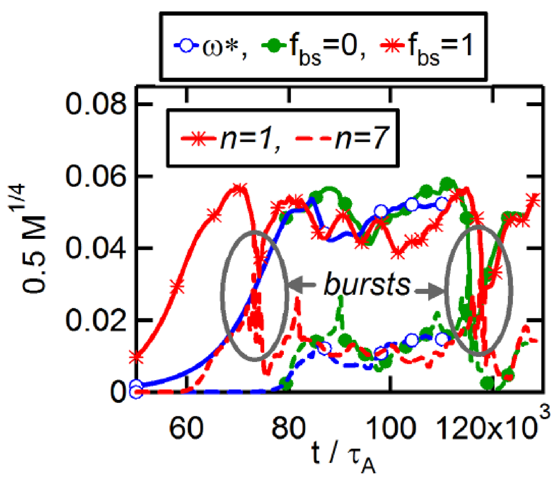

Fig.2 : Island size; bursty behaviour at low χ, ν with neoclassical model.

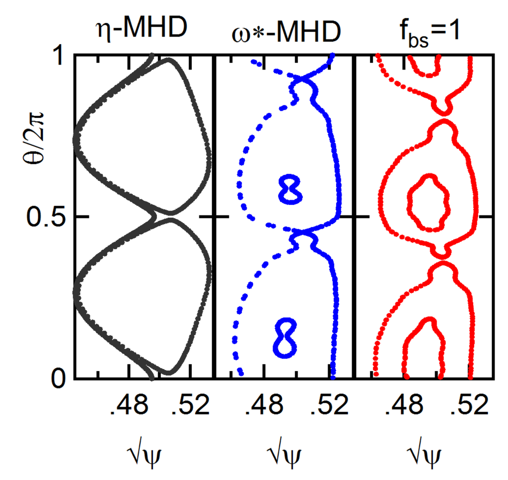

Fig.3 : Island shape with resistive, drift and neoclassical MHD models.

Comparison with Rutherford approach

- Effect of bootstrap current on saturation mitigated by ExB flow perturbation
- Measured by correlation $R_{bs}(p)$ between bootstrap and pressure perturbations
- Correlation $R_{bs}(p)$ increases with neoclassical friction μ_i and with island size [fig.4]
- In Rutherford representation, f_{bs} *[=1 for reference case]* replaced by $R_{bs}(p)f_{bs}$
- Still weaker effect compared with Rutherford prediction, even for an ad-hoc implementation of the bootstrap J_{bs}~∇p where $R_{bs}(p)=1$

Application to Neoclassical Tearing Mode triggering on Asdex-Upgrade equilibrium

- Correlation $R_{bs}(p)$ varied by changing $\chi_{//}$ (~pressure flattening inside the island)
- (3,2) NTM could be triggered for a seed W_{seed}~4%

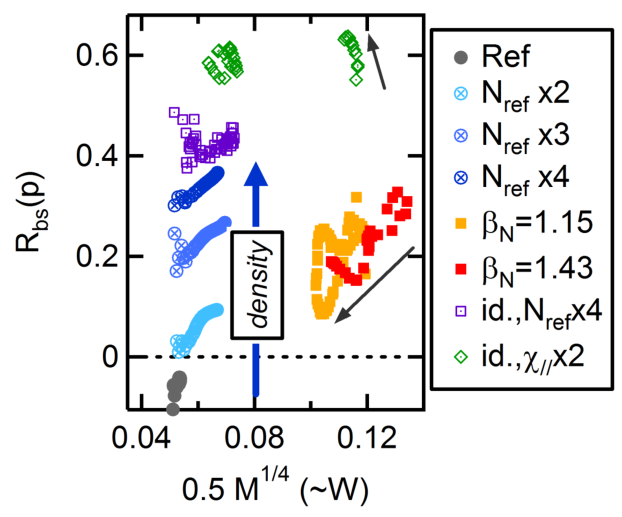

Fig.4 : Correlation between bootstrap & pressure perturbations vs island size.

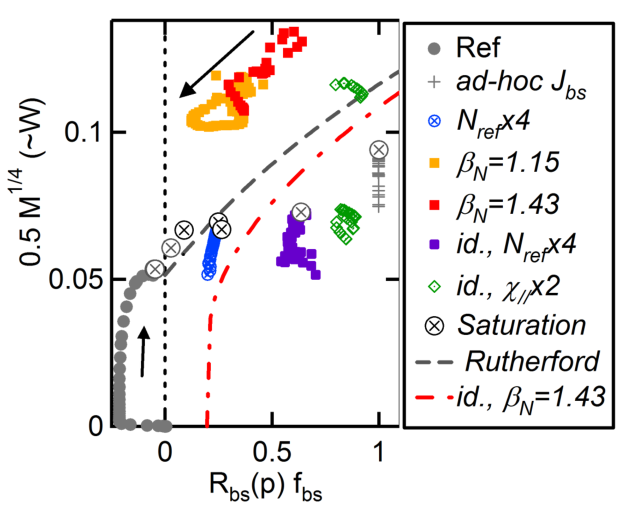

Fig.5 : Island size vs effective bootstrap current

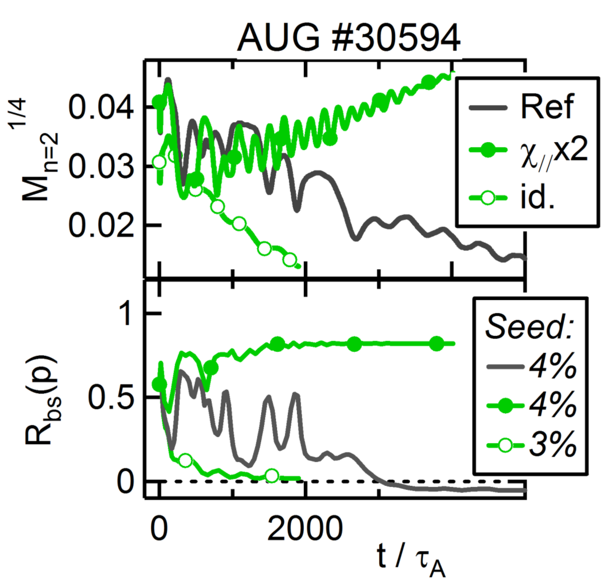

Fig.6 : (3,2) NTM triggering by changing $R_{bs}(p)$ via $\chi_{//}$.

Island control by ECCD: validation & 3D effects

Implementation of a 3D RF current source (J_s) in XTOR [5]

- Propagation along field lines through parallel diffusion: quasi-homogeneous

$$\frac{\partial J_{RF}}{\partial t} = \nu_f(J_s - J_{RF}) + \chi_\perp^{RF}\nabla_\perp^2 J_{RF} + \chi_\parallel^{RF}\nabla_\parallel^2 J_{RF}$$

Validation of stabilization efficiency η_{RF} with respect to analytical theory

- Recovers predicted dependence vs source width δ_{RF} & vs misalignment [fig.7]
  - *But reduction of η_{RF} found in non-circular cross sections*

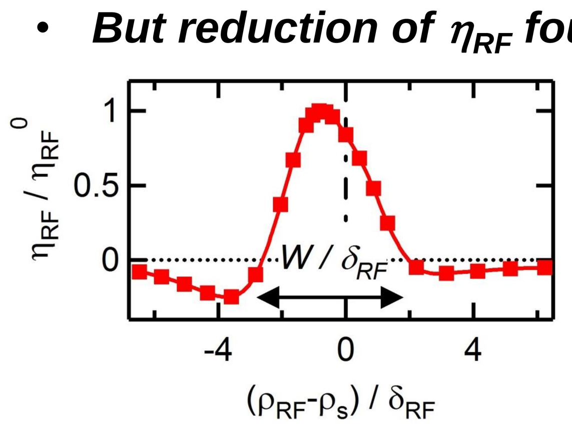

Fig.7:Stabilization efficiency vs misalignment.

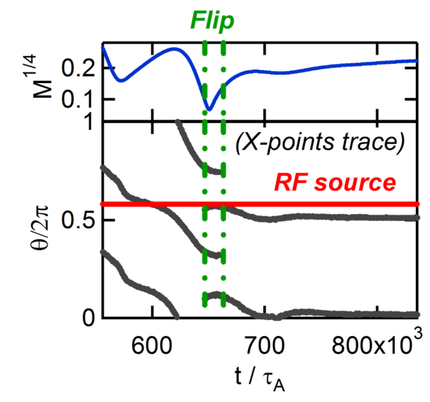

Fig.8 : θ - position of X-points vs time during flip instability.

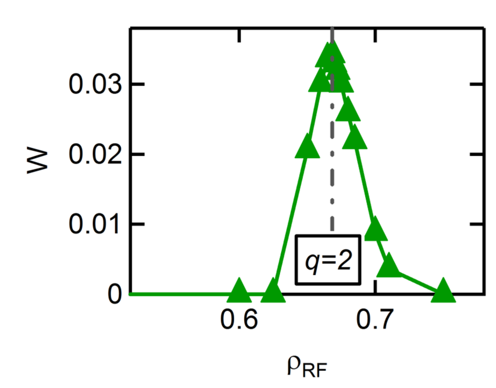

Fig.9 : RF-driven island size vs RF deposition (I_{RF}/I_p=0.75%).

Specific features with a 3D source : island adjusts its phase to enhance its growth

- Flip instability [6]: the X-point sets in close to the RF source (destabilizing) [fig.8]
- RF-driven island : when close to a resonant surface, the RF current filament forms the X-point of an island [fig.9]

Island control by ECCD: evaluating various strategies

- A basic controller has been implemented for radial sweep and modulation
- Radial sweep aimed at mitigating misalignment risk [7]: successfully tested on TCV and Asdex-Upgrade during the last MST1 campaigns [see overviews, this conf.]
- Modulation aimed at mitigating low efficiency associated with broad RF deposition
- Evaluation of best strategy using the resistive MHD model [8]

Preemption

- Risk due to misalignment [9]: mitigation by radial sweep at the cost of a larger I_{RF} [fig.10]

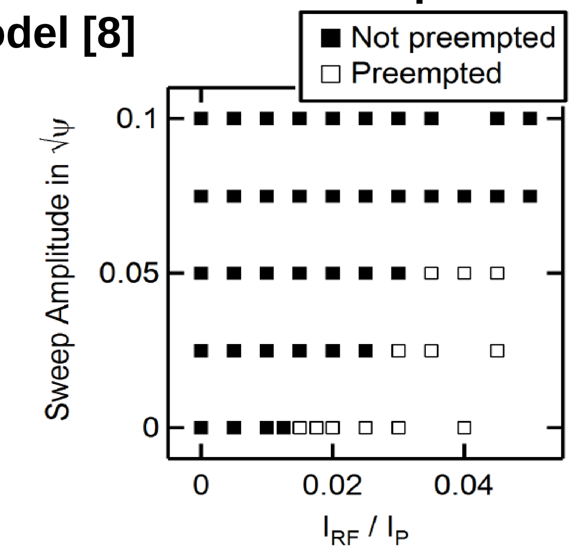

Fig.10 : Preemption capability as a function of RF current and sweep amplitude

Stabilization (broad source, δ_{RF}/W=1.4) [fig.11]

- Radial sweep : island reduction without misalignment risk, but less efficient than well positionned fixed source
- Combined with modulation : full stabilization obtained
- Alternate modulation with the FADIS (FAst DIrectional Switch) method uses 2 antennae to obtain a nearly continuous O-point deposition [10]
- Quantification by a gain G and a characteristic time T_{min}

$$G = \frac{W_{sat} - W_{min}}{W_{sat} - W_0}$$

- W_{sat} : island size without control
- W_{min}: minimum width obtained
- W_0 : minimum width for fixed, CW source
- T_{min} : time for reaching W_{min}

- Overview of stabilization strategies [fig.12]
  - Island control achieved without misalignment risk
  - Large gain for modulation techniques
  - Control time scale reduced with the FADIS alternate modulation scheme

Thin RF source (δ_{RF}/W=0.7) : results qualitatively similar, but no advantage to use modulation techniques (G~1) (see [8])

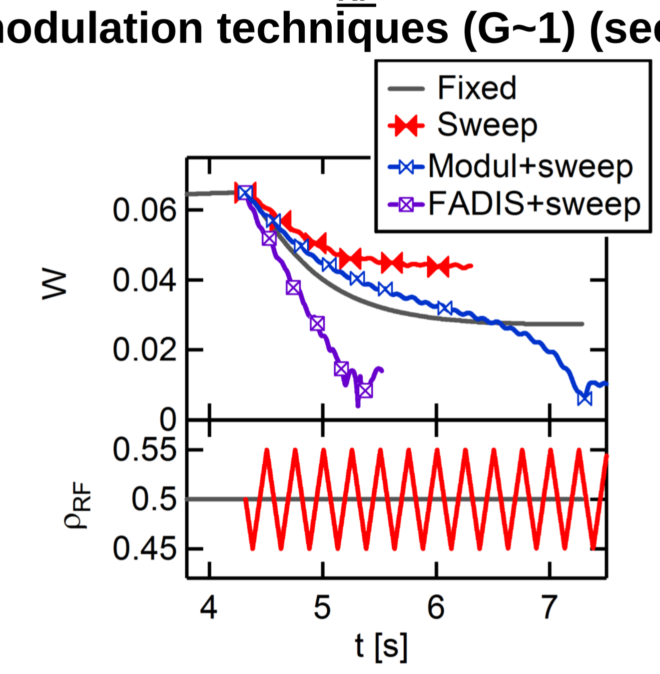

Fig.11 : Island width evolution following different strategies (top); RF deposition during the sweep (bottom).

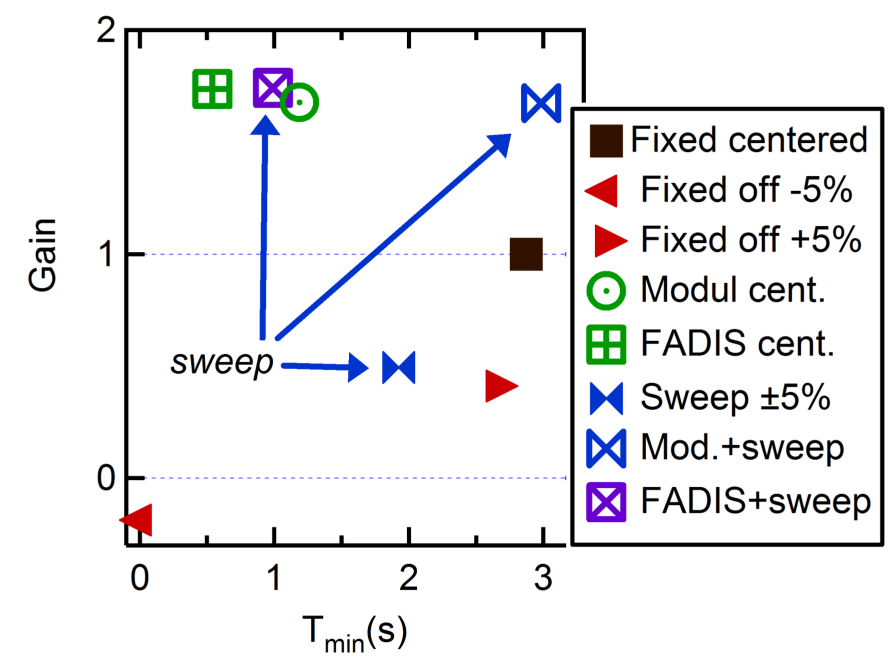

Fig.12 : Gain as a function of characteristic control time T_{min}.

References

[1] H. Lütjens et al, J. Comp. Phys. **229** (2010), 8130.
[2] P. Maget et al, Nucl. Fus. **56** (2016) 086004;
N. Mellet et al, Nucl.Fus. **53** (2013) 053022
[3] S. Hirshman et al, Nucl. Fus. **21** (1981) 1079
[4] O. Sauter et al, Phys. Plasmas 6, 2834 (1999)
[5] O. Février et al, PPCF 58 (2016) 045015
[6] D. Borgogno et al, Phys. Plasmas **21** (2014) 060704
[7] F. Felici et al, Nucl. Fusion **52** (2012) 074001
[8] O. Février et al, Varenna 2016 (sub. to PPCF)
[9] A. Pletzer et al, Phys. Plasmas **6** 1589 (1999)
[10] W. Kasparek Nucl. Fusion **56** (2016) 126001

Acknowledgements

Work carried out within the framework of the EUROfusion Consortium ; funding from the Euratom research and training programme 2014-2018 (grant agreement No 633053) ; from Agence Nationale pour la Recherche (ANR-14-CE32-0004-01). The views and opinions expressed herein do not necessarily reflect those of the European Commission.

Numerical resources provided by GENCI (project no. 056348), Mésocentre of Aix-Marseille University (project no. 16b009), IFERC-CSC (project MaCoToP)